Contribution No. 4538 from the Central Research and Development Department, Experimental Station, E. I. du Pont de Nemours and Company, Inc., Wilmington, Delaware 19898, and Contribution from the Department of Physics, Colorado School of Mines, Golden, Colorado 80401

X-ray Photoelectron Mössbauer, Magnetic, and Electrical Conductivity Study of $SnS_2\{CoCp_2\}_{0.31}$

Dermot O'Hare,*[†‡] Wolfram Jaegermann,[†§] D. L. Williamson,[∥] Fumio S. Ohuchi,[†] and B. A. Parkinson[†]

Received October 2, 1987

Intercalation of SnS_2 with $CoCp_2$ (Cp = η-C_5H_5) under mild conditions leads to the formation of $SnS_2\{CoCp_2\}_{0.31}$. Its physical properties have been investigated with a variety of techniques. X-ray photoelectron spectroscopy reveals the presence of Co^{3+}, Co^{2+}, Sn^{4+}, and probably Sn^{2+}. Electron paramagnetic resonance spectra showed the presence of radicals with g values close to those observed for cobaltocene intercalated into $CdPS_3$. Magnetic measurements showed that the sample obeyed the Curie–Weiss expression between 4 and 300 K with $\Theta = -9.17$ K, and $\mu_{eff} = 0.12\ \mu_B$. ^{119}Sn Mössbauer spectroscopy revealed the presence of a resonance assignable to a reduced tin site that could be formulated as Sn^{2+} and an integrated Sn^{2+}:Sn^{4+} ratio of 0.11. Diffuse reflectance spectroscopy showed the onset of a broad absorption in the near-IR region at 0.6 eV, in addition to the band gap of SnS_2 at 2.1 eV. Electrical conductivity showed that the intercalated material is 200 times more conductive than the unreacted host but still showed semiconducting behavior with an activation energy $E_a = 0.11$ eV, similar to that of unintercalated SnS_2. The stoichiometry of the intercalated material can best be described as $(Sn^{4+}_{0.9}Sn^{2+}_{0.1})S_2\{[Co^{3+}Cp_2]^+_{0.2}[Co^{2+}Cp_2]_{0.1}\}$ which is remarkable due to the multiple mixed valency of the material.

Introduction

Many of the transition-metal dichalcogenides (MX_2) crystallize in a layered structure in which planes of nearly octahedral or trigonal prismatic coordinated metal atoms (M) are bound by parallel planes of hexagonally packed chalcogen atoms (X).[1] The macroscopic structure is built from lamellar stacks of XMX repeat units with a characteristic interstitial space or van der Waals gap between adjacent chalcogen atom planes.

The layered structure of MX_2 lattices permits a variety of atoms or molecules to be intercalated into the van der Waals gap.[2,3] Considerable research on the intercalation reactions of these lattices indicates that in many cases a process involving transfer of electrons from the intercalate to the host lattice occurs.[4] In some cases donor–acceptor interactions between the d orbitals of the host and lone-pair orbitals on the intercalate are implicated.[5]

Dines has previously reported the intercalation of cobaltocene into SnS_2 but reported no details of the physical properties of the obtained material.[6] Recently cobaltocene has also been intercalated into $SnSe_2$, but again no detailed studies of the physical properties were reported.[7] Cleary and Francis[8] studied the EPR behavior of oriented single crystals of cobaltocene intercalated $CdPS_3$ and found anisotropic behavior. An EXAFS study of the cobaltocene intercalation compound of $Mn_{0.83}PS_3$ has also been reported as well as its magnetic properties.[9]

Photoemission spectroscopy can yield interesting insights into the electronic structure of intercalated materials allowing inference of the extent of charge transfer from guest to host from core-level binding energy shifts and from the analysis of the electronic structure of the valence band.[10] However, up until now very few papers have been published where X-ray or UV photoemission spectroscopy (XPS or ESCA and UPS, respectively)[11–14] have been used for the characterization of intercalated layered metal dichalcogenides.

In light of the interesting physical properties of many guest–host systems and the lack of a complete characterization of any such compounds, we report XPS, optical, Mössbauer, EPR, magnetic, and electrical conductivity studies of the $SnS_2\{CoCp_2\}_{0.31}$ (Cp = $C_5H_5^-$) intercalation compound.

Experimental Section

General Information. All manipulations were carried out under an atmosphere of dinitrogen in a Vacuum Atmospheres Dri-Box. All solvents were predried over molecular sieves and then distilled from sodium (dimethoxyethane) or CaH_2 (acetonitrile).

The X-ray photoelectron spectroscopy measurements were performed in an UHV multitechnique chamber with monochromatized X-rays (Al Kα). The XPS system was constructed by Surface Science Lab, Inc., and was equipped with a computer system (HP 9836) for data aquisition and manipulation. One special advantage of this system is the capability to probe small areas (300 μm). Further details of the system configuration are given elsewhere.[15] The spectrometer was calibrated with clean evaporated Au and Cu samples. The resolution achieved was about 0.9 eV. The measurements of $CoCp_2$ and $[CoCp_2]^+[PF_6]^-$ were performed in a Kratos XPS system with specimen cooling equipment. Mg Kα radiation was used as an excitation source leading to a resolution of 0.9 eV.

The ^{119}Sn Mössbauer measurements were made in the constant acceleration mode with a $Ca^{119m}SnO_3$ 5 mCi source. Measurements were made with both the source and the absorber at liquid-nitrogen temperature. Absorbers were made from 10 mg quantities of $SnS_2\{CoCp_2\}_{0.31}$ crystals by grinding them into a fine powder and dispersing the powder into an inert binder (powdered sucrose). One sample was ground under liquid nitrogen, and a second was ground in air. A pure sample of SnS_2 was also measured for comparison. Precision isomer shifts (δ) and line widths (Γ) (full width at half-maximum) were obtained by least-squares fitting of sums of Lorentzian lines to the 256 data points of each spectrum and by performing periodic velocity calibrations. The zero of velocity was established with a $CaSnO_3$ absorber (same compound as the source), and all isomer shifts are reported relative to this standard at room temperature.

ESR spectra were recorded on an IBM/Bruker ER 200 D-SRC spectrometer. Magnetic susceptibility data were recorded by using the Faraday technique from 3 to 300 K. Single-crystal electrical conductivity measurements were recorded from 180 to 300 K with a computer-controlled liquid-N_2-cooled cryostat and the four-point probe method.

[†] E. I. du Pont de Nemours and Co., Inc.
[‡] On leave from the Inorganic Chemistry Laboratory, University of Oxford, Oxford OX1 3QR, England.
[§] On leave from the Hahn Meitner Institute, Glienicker Str. 100, 1000 Berlin 39, W. Germany.
[∥] Colorado School of Mines.

(1) Hooter, E., Ed.; *Physics and Chemistry of Materials with Layered Structure*; D. Reidel: Dordrecht, The Netherlands, 1976; Vol. 1.
(2) Levy, F. A., Ed.; *Physics and Chemistry of Materials with Layered Structure*; D. Reidel: Dordrecht, The Netherlands, 1979; Vol. 6.
(3) Whittingham, M. S.; Jacobsen, A. J., Eds.; *Intercalation Chemistry*; Academic: New York, 1982.
(4) Schöllhorn, R. *Comments Inorg. Chem.* **1983**, *2*, 271.
(5) Schöllhorn, R. *Angew. Chem.* **1980**, *92*, 1015.
(6) Dines, M. B. *Science (Washington, D.C.)* **1975**, *188*, 1210.
(7) Benes, L.; Votinsky, J.; Lostak, P.; Kalousova, J.; Klikorka, J. *Phys. Status Solidi* **1985**, *89*, K1.
(8) Cleary, D. A.; Francis, A. H. *J. Phys. Chem.* **1985**, *89*, 97.
(9) Michalowicz, A.; Clement, R. *J. Inclusion Phenom.* **1986**, *4*, 265.
(10) Briggs, D., Ed. *Handbook of X-ray and Ultraviolet Photoelectron Spectroscopy*; Heyden: London, 1977.
(11) Williams, R. H. *Phys. Status Solidi* **1978**, *88*, K157.
(12) Bach, B.; Thomas, J. M. *J. Chem. Soc., Chem. Commun.* **1972**, 301.
(13) Eppinga, R.; Sawatsky, G. A.; Haas, C.; von Bruggen, C. F. *J. Phys. C* **1976**, *9*, 3371.
(14) Sternberg, H. I.; Hughes, H. P. *J. Phys. C* **1987**, *20*, 297.
(15) Chaney, L. *Recent Development in Spatially Resolved ESCA*; Surface Science Lab Publication: Mountain View, CA, 1985.

0020-1669/88/1327-1537$01.50/0

Table I. Typical Stoichiometries and Lattice Expansions for $CoCp_2$ Intercalation into Layered Materials

host	reacn conditions: temp, °C	reacn conditions: time, days	stoichiometry	Δc, Å	ref
TiS_2	23	19	0.20	5.55	3
ZrS_2	100	4	0.27	5.35	3
TaS_2	23	24	0.25	5.47	3
$SnSe_2$	125	14	0.33	5.37	7
SnS_2	23	1	0.31	5.35	this work

Diffuse reflectance measurements were recorded on an Cary 2300 spectrometer.

Experimental Details. Synthesis of SnS_2. SnS_2 was prepared by reaction of high purity elements (>99.999%) in evacuated sealed quartz ampules at 750 °C via the reported procedure.[16] Single crystals were grown in quartz ampules loaded with SnS_2 and 5 mg/cm^3 of I_2 as a transport agent. The ampules were placed in a two-zone tube furnace with a temperature of 780 °C at the hot zone and 740 °C at the cool zone for periods of several days. Typical crystals were hexagonal platelets of dimension 4 × 4 × 0.01 mm.

Synthesis of $SnS_2\{CoCp_2\}_{0.31}$. Crystalline SnS_2 (1.4 g; 7.8 mmol) was added to a solution of $CoCp_2$ (1.85 g, 10.2 mmol) in glyme (50 cm^3); the bright yellow color the SnS_2 quickly disappeared, yielding a bluish metallic luster. The suspension was stirred at room temperature (higher temperatures accelerate the reaction but the magnetic measurements indicate higher decomposition levels) for 4 days to ensure that the largest crystals had completely reacted. After 4 days the suspension was filtered and the solid washed with glyme (4 × 20 cm^3) until the washings were colorless and dried in vacuo. The homogeneity of the sample was confirmed by powder X-ray diffraction, which showed the disappearance of some lines associated with SnS_2 and the characteristic increase in the interlayer spacing of 5.35 Å.[6] The stoichiometry was confirmed by elemental analysis. Found (calcd) for $SnS_2Co_{0.31}C_{3.10}H_{3.10}$: C, 15.46 (15.42); H, 1.42 (1.29).

Sample Preparation for XPES Studies. Single crystals of *n*-type SnS_2 (phosphorus doped) and intercalated SnS_2 were attached with one van der Waals face to an Al sample holder via conductive Ag epoxy and allowed to dry for 12 h under a nitrogen atmosphere. Clean van der Waals surfaces were produced by cleaving the crystals under ultrahigh vacuum (UHV) via application of sticky tape to the exposed surface and peeling off a layer from the crystal.

$CoCp_2$ was sublimed via a leak valve from a heated glass furnace onto an indium sample holder kept at 77 K. No contaminants were present as indicated by the XP spectrum, and only negligible charging effects occurred. $[CoCp_2]^+[PF_6]^-$ powder was handled under a nitrogen atmosphere in a glovebag connected to the spectrometer entrance port. The sample was pressed into a very thin layer onto indium and immediately transferred into the UHV system. Charging and contamination effects were also absent in this material. Therefore in all cases the binding energy reference point (E_B = 0 eV) was the Fermi edge of metallic samples, and no additional corrections with respect to C(1s) were performed.

Results and Discussion

$CoCp_2$ can be intercalated under mild conditions into single crystals of n-type SnS_2 with a resultant stoichiometry of $SnS_2\{CoCp_2\}_{0.31}$. This stoichiometry is consistent with the value of 0.29 found previously[6] and is close to the value of 0.33 measured for the intercalation of cobaltocene into $SnSe_2$ (Table I).[7] The rate of reaction seems to be strongly dependent on the choice of solvent; with dimethoxyethane, the bright yellow color of SnS_2 is quickly transformed into a metallic luster on contact with the $CoCp_2$ solution while with CH_3CN, complete reaction required temperatures of ca. 70 °C for 3 days. Complete intercalation of relatively large single crystals (4 × 4 × 0.01 mm) is complete after 3–4 days at room temperature with dimethoxyethane.

The size of the $CoCp_2$ molecule and the magnitude of the interplanar expansion suggest that the intercalate is oriented with the C_5 axis parallel to the van der Waals layers (Figure 1). Wide-line NMR studies by Silbernagel on the intercalation of $CoCp_2$ into TaS_2 also indicate this equilibrium orientation.[17] For example, the layer spacing of TaS_2 was seen to increase as larger

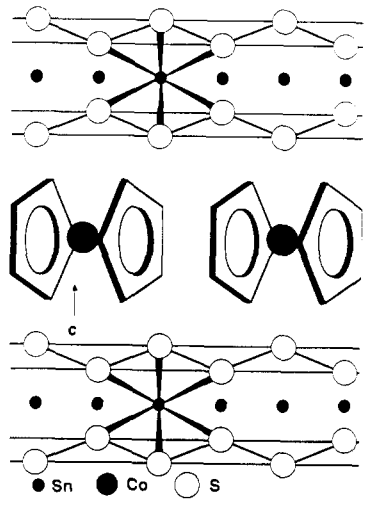

Figure 1. Schematic representation of the intercalation of $CoCp_2$ into SnS_2.

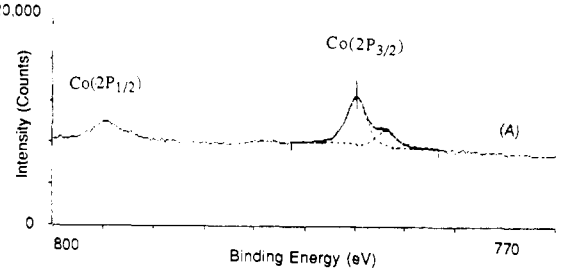

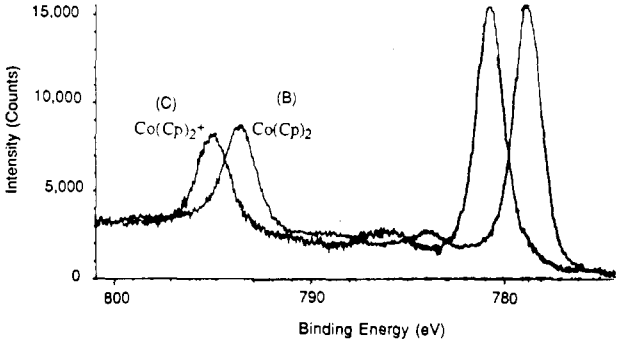

Figure 2. Co binding energy region of the XPS spectra of (A) $SnS_2\{CoCp_2\}_{0.31}$, (B) $CoCp_2$, and (C) $[CoCp_2]^+PF_6^-$.

substituents were added to the cyclopentadienyl ring. Surprisingly, we have been unable to intercalate $Co(C_5Me_5)_2$ into SnS_2 by direct reaction. Since this is a more thermodynamically favored reaction, the increased steric bulk of the C_5Me_5 rings must be kinetically limiting the reaction.

X-ray Photoelectron Spectra. The XPS-results obtained for the core levels of SnS_2 and $SnS_2\{CoCp_2\}_{0.31}$ are summarized in Figure 2 and Table II. The main Sn and S emission peaks show no change in their binding energies due to intercalation. Only slight increases in peak widths are obtained.

A weak additional Sn emission (ca. 4% of the main emission peak) appears at lower binding energy (ΔE_B = 1 eV) and can be assigned to a reduced tin species.[18] Similar values have been obtained for the intercalation of Cu into SnS_2.[19] This assignment is based on the measured binding energy value and must be treated with caution, since the binding energy shift may be due to movement of E_F within the band gap of the semiconductor.

(16) Rimmington, H. P. B.; Baldwin, A. A.; Tanner, B. K. *J. Cryst. Growth* **1972**, *15*, 51.
(17) Silbernagel, B. G. *Chem. Phys. Lett.* **1975**, *34*, 298.
(18) Muilenberg, G. E. *Handbook of X-Ray Photoelectron Spectroscopy*; Perkin Elmer: Eden Praine, NY, 1979.
(19) Jaegermann, W.; Ohuchi, F. S.; Parkinson, B. A., submitted for publication in *Surf. Sci.* submitted.

Table II. Summary of the Important XPS Binding Energy Values (eV)

sample	$Sn(4d_{5/2})$	$Sn(3d_{5/2})$	$S(2p_{3/2})$	$Co(2p_{3/2})$	C(1s)
SnS_2[a]	26.1 (3.4)	487.0 (27.5)	162.0 (3.8)		
$SnS_2\{CoCp_2\}_{0.31}$[a]	26 (3.1)	486.9 (24.6)	161.9 (3.2)	780.2 (1.6)	285 (1.4)
	25 (0.1)	485.8 (1)		781.9 (4.6)	286.1 (6.5)
$SnS_2\{CoCp_2\}_{0.31}$[b]	26.0 (2.5)	487.0 (22.2)	161.9 (1.8)	780.4 (1.1)	
	26.7 (1.4)	487.8 (5)		781.9 (8.2)	
$CoCp_2$[c]				779.3 (3.0)	284.9 (3.3)
$[CoCp_2]^+[PF_6]^-$[d]				782.1 (2.7)	285.9 (3.2)

[a] UHV cleaved. [b] Air oxidized. [c] Sublimed onto indium at −196 °C. [d] Pressed onto indium.

The intercalated material shows two different $Co(2p_{3/2})$ emission peaks separated by 1.8 eV and two C(1s) peaks separated by 1 eV. The intensity ratios of the low-binding-energy peaks to the high-binding-energy peaks are usually found to be 1:2.8 and 1:2, respectively. The intensity ratios for different crystals tend to be scattered, reaching in extreme cases a value of about 1:1. The Co/Sn ratio of 0.45 is calculated without considering the exponential decay of emission intensity with escape depth and is in reasonable agreement with the chemical analysis. The Co:C peak intensity ratio is 1:10 for the high-energy peaks and a little larger for the low-energy peaks. This suggests that small quantities of the solvent are also intercalated since the cleavage was performed in UHV and surface contamination can be excluded. A small O(1s) peak is obtained in all spectra of intercalated SnS_2, supporting the hypothesis that a small quantity of glyme may be present.

The existence of two different Co and C peaks suggests that upon intercalation two different organocobalt species are present. The difference in binding energies for the $Co(2p^3/_2)$ bands clearly suggests that the cobalt species are Co^{2+} and Co^{3+}. Therefore the XP spectra of $CoCp_2$ and $[CoCp_2]^+[PF_6]^-$ were measured for comparison (Figure 2 and Table II). The binding energies obtained are in good agreement to the values measured for $SnS_2\{CoCp_2\}_{0.31}$ and point clearly to the fact that both $Co^{2+}Cp_2$ and $[Co^{3+}Cp_2]^+$ are intercalated (Table II).

It is generally accepted that the metallocenium ion is formed on intercalation into these layered hosts;[3,4] our conclusion that we have also intercalated neutral molecules is unexpected. Although we cannot eliminate accidental degenercies of binding energy shifts between $CoCp_2$ and some other undefined decomposition product, we can eliminate other likely products such as CoS. The XPS data and the other physical measurements (vide infra) make for a convincing argument that the additional species is $CoCp_2$.

The valence band spectra of SnS_2 and $SnS_2\{CoCp_2\}_{0.31}$ and their difference spectrum are shown in Figure 3. The valence band spectra of $CoCp_2$ and $[CoCp_2]^+[PF_6]^-$ are also given for comparison. The difference spectrum shows characteristic features at 3.5 (sh), 4.5, 6.0, 8.9 (v br), 13.1, and 17.6 eV. The difference spectrum of SnS_2 and $SnS_2\{CoCp_2\}_{0.31}$ resembles the summation of the valence band spectra due to $CoCp_2$ and $[CoCp_2]^+[PF_6]^-$ with the correct weighting factors. The first peaks between 3 and 7 eV are assigned to Co 3d electron states and the emissions ca. 9 and 13 eV are related to η-Cp π-bonding states in agreement with the literature data[20] from gas-phase photoemission measurements.

It is interesting to note that the valence band spectrum of $SnS_2\{CoCp_2\}_{0.31}$ shows emission intensity tailing off to the Fermi level (binding energy reference energy = 0.0 eV). This indicates filled electron states close to the conduction band that can be assigned to the partially occupied Co π^*-antibonding level in $CoCp_2$ and to occupied Sn 5s conduction band derived states. Whereas pure SnS_2 shows a distance of 1.7 eV between the valence band maximum and the Fermi level as expected for the n-type semiconductor with a band gap of 2.2 eV.

The unintercalated SnS_2 (0001) surface is inert to oxidation by air[19] whereas the intercalated material is air sensitive. Oxidation of the sample can clearly be seen by the shift of the core levels of the substrate as well as Co peaks after a 12 h exposure to air (Table II). The substrate emissions show additional high-energy peaks that clearly indicate the formation of SnO_2 and SO_4^{2-}.[18] Correspondingly the O(1s) peak of oxides (E_B = 531.5 eV) is strongly increased and the S:Sn atomic ratio is decreased. The higher binding energy Co peak gains in intensity relative to the lower binding energy peak, indicating oxidation of the remaining $CoCp_2$. As a consequence, the valence band spectrum shows mostly the features of $[CoCp_2]^+$ and the extra emission intensity due to the transferred conduction band electrons is strongly diminished.

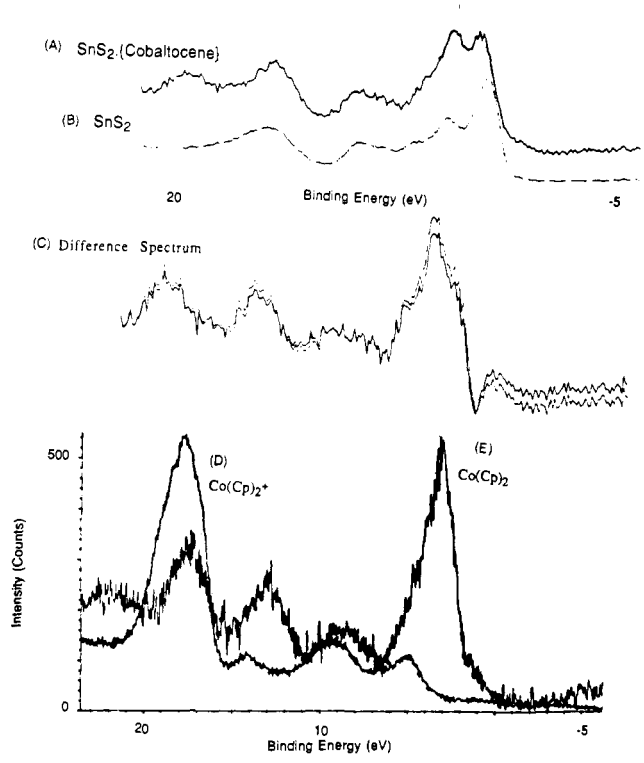

Figure 3. Valence band region of the XPS spectrum of (A) $SnS_2\{Co(\eta\text{-}Cp)_2\}_{0.31}$, (B) the XPS spectrum of SnS_2, (C) the difference spectrum (A − B), (D) the XPS spectrum of $CoCp_2$, and (E) the XPS spectrum of $[CoCp_2]^+[PF_6]^-$.

Diffuse Reflectance Measurements. The diffuse reflectance spectra of crystalline samples of SnS_2 and $SnS_2\{CoCp_2\}_{0.31}$ were measured between 200 and 1950 nm (Figure 4). Both samples show an absorbance associated with the 2.1-eV (590-nm) band gap of the semiconductor. In addition, the spectrum of $SnS_2\{CoCp_2\}_{0.31}$ shows a broad absorbance tailing off at 1950 nm (0.66 eV). This broad feature arises from the creation of many new electron states close to the Fermi level, which was also observed in the valence band region of the XPS spectra.

Magnetic Susceptibility Measurements. The molar magnetic susceptibility (χ_M) of $TaS_2\{CoCp_2\}_{0.25}$ was found to be $+88 \times 10^{-6}$ emu mol^{-1}, somewhat less than that of pure 2H-TaS_2,[21] and was independent of temperature down to 2 K. The loss of the local moment is consistent with the complete oxidation of the guest by

(20) Cauletti, C.; Green, J. C.; Kelly, M. R.; Powell, P.; Van Tilborg, J.; Robbins, J.; Smart, J. *J. Electron Spectrosc. Relat. Phenom.* **1980**, *19*, 327.

(21) Gamble, F. R.; Thompson, A. H. *Solid State Commun.* **1978**, *27*, 279.

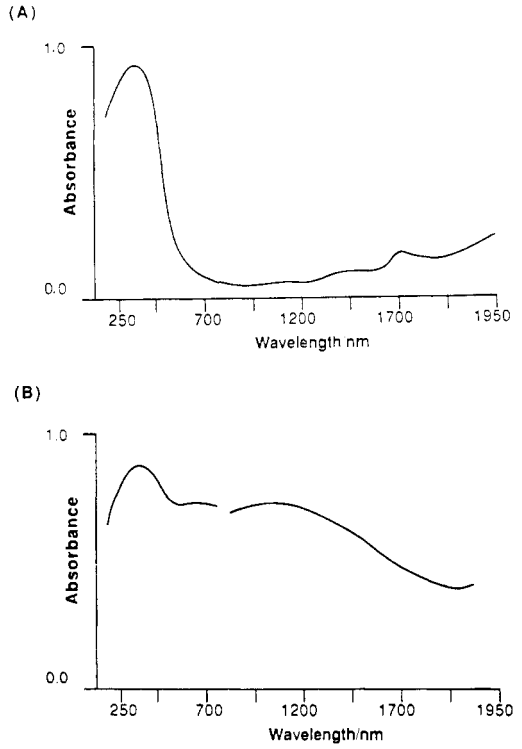

Figure 4. Diffuse reflectance spectra of (A) n-doped SnS_2 and (B) $SnS_2\{CoCp_2\}_{0.31}$.

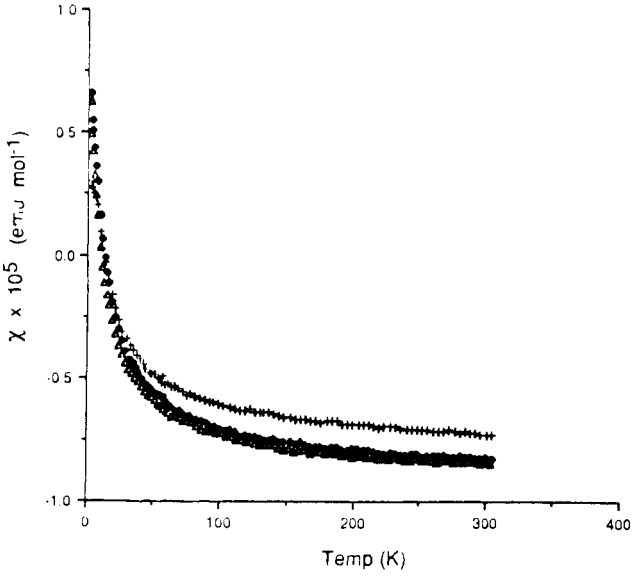

Figure 5. Plot of χ vs T for $SnS_2\{CoCp_2\}_{0.31}$ at various magnetic fields: (□) 19.5 kG; (♦) 18.5 kG; (+) 15.8 kG.

the TaS_2. Since $CoCp_2$ is paramagnetic with $\mu_{eff} = 1.81\ \mu_B$ and $[CoCp_2]^+$ is diamagnetic, the ultimate fate of the electron within the band structure is unknown.

The magnetic susceptibility of $SnS_2\{CoCp_2\}_{0.31}$ was measured between 4 and 300 K, at magnetic field strengths of 15.8, 18.5, and 19.5 kG (Figure 5). The magnetic field dependence of the magnetic susceptibility can be clearly seen in the room-temperature data and is indicative of trace amounts of a ferromagnetic impurity. The amount of impurity, presumably cobalt metal (arising from some decomposition of $CoCp_2$) was found to vary from sample to sample. The lowest temperatures syntheses gave the smallest amounts of this impurity.

A plot of χ vs $1/H$ (H = field) for the room temperature data was found to be linear (Honda analysis). The slope of this plot gives a value for the contribution to the total susceptibility due to the ferromagnetic impurity. This analysis indicated that the total ferromagnetic impurity (M_{Co} = 0.95 emu G mol^{-1}) was 24 ppm. This correction was applied to the measured susceptibility at each field strength and at all temperatures. The corrected magnetic susceptibility was field independent within experimental error over all temperatures measured.

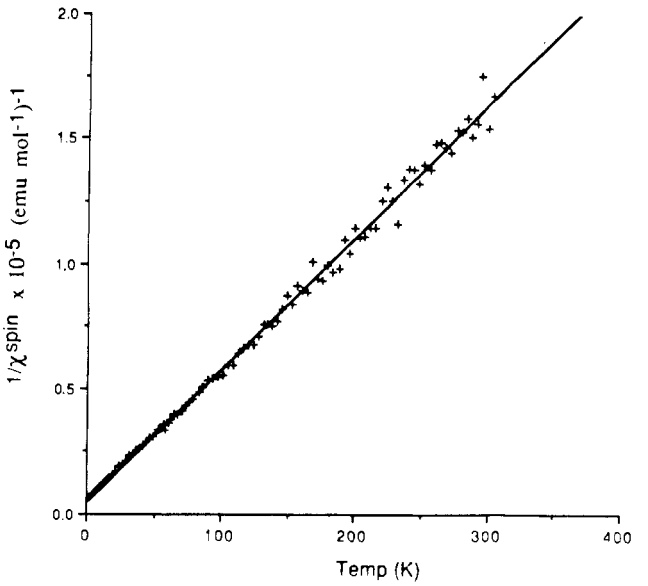

Figure 6. Plot of χ^{-1} vs T for $SnS_2\{CoCp_2\}_{0.31}$.

Table III. Selected **g** Tensors for $CoCp_2$ Diluted in Different Host Systems

host	sample	$g_\parallel$	$g_\perp$	ref
$FeCp_2$	powder	1.69	1.81	22
$Mg(C_5H_4Me)_2$	frozen sol	1.69	1.85	22
$Cr(C_6H_6)(CO)_3$	powder	1.724	1.93	22
$CdPS_3$	single cryst	2.00	1.96	8
SnS_2	powder	2.09	1.99	this work

A subsequent plot of $1/\chi_{cor}$ vs T (Figure 6) showed that the sample obeyed the Curie–Weiss expression between 4 and 300 K with a values of Θ = −9.17 K, and $\mu_{eff} = 0.12\ \mu_B$.

Although the effective magnetic moment is small it corresponds to ca. 22% of the intercalated organometallic material being $CoCp_2$ ($S = {}^1/_2$), which is close to the value of ca. 35% found from the XPS experiments. The negative value of Θ indicates that there may be significant intermolecular antiferromagnetic coupling.

Electron Paramagnetic Resonance Experiments. Crystalline samples of $SnS_2\{CoCp_2\}_{0.31}$ exhibit an EPR spectrum at temperatures between 4 and 300 K (Figure 7). The spectra are sample dependent, and there seems to be a strong dependence on the orientation of the crystals in the EPR cavity. However, the spectrum of a finely powdered sample at 4.7 K can be analyzed in terms of an axially symmetric powder spectrum with $g_\perp = 2.092$ and $g_\parallel = 1.994$. The **g** tensors are not in agreement with the published values for $CoCp_2$ diluted in diamagnetic hosts (Table III); however, the **g** tensors of ^2E ground-state radicals are very host dependent.[22] Single-crystal EPR studies on $CdPS_3\{CoCp_2\}_{0.35}$ showed signals due to unoxidized $CoCp_2$ with $g_\perp = 2.00$ and $g_\parallel = 1.96$.[8] The authors[8] note that the spectrum is very dependent on orientation.

We can conclude that the intercalate contains metal-based radicals, the line shape of the powder spectrum at 4 K is most consistent with axial symmetry, and the **g** tensors are close to those reported for $CoCp_2$ in $CdPS_3$.

Electrical Conductivity Measurements. Electrical conductivity (σ) on single crystals of SnS_2 and $SnS_2\{CoCp_2\}_{0.31}$ were measured between 180 and 300 K by using the four-point probe method (Figure 8). Both samples show classical semiconductor behavior over the complete temperature range. No hysteresis effects were observed upon sample cooling or heating. Plots of ln (σ) vs $1/T$ were found to be linear, yielding activation energies (E_a) of 0.14

(22) Ammeter, J. H. *J. Magn. Reson.* **1978**, *30*, 299.

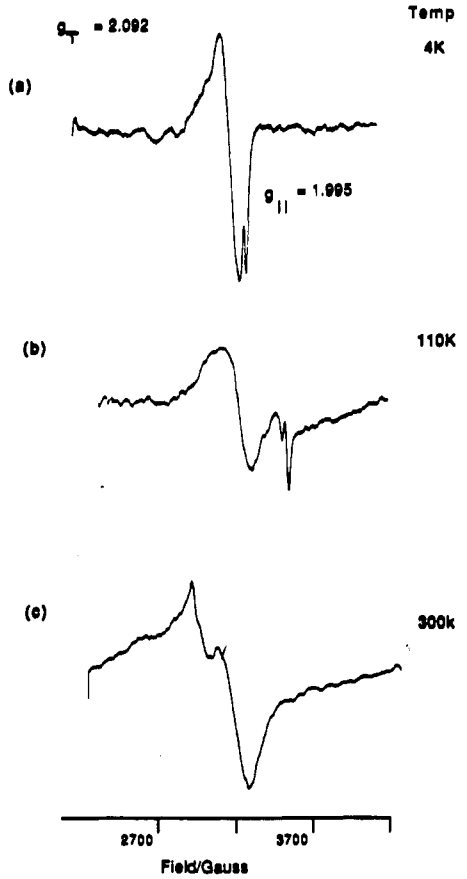

Figure 7. Variable-temperature EPR spectra of powdered $SnS_2\{CoCp_2\}_{0.31}$.

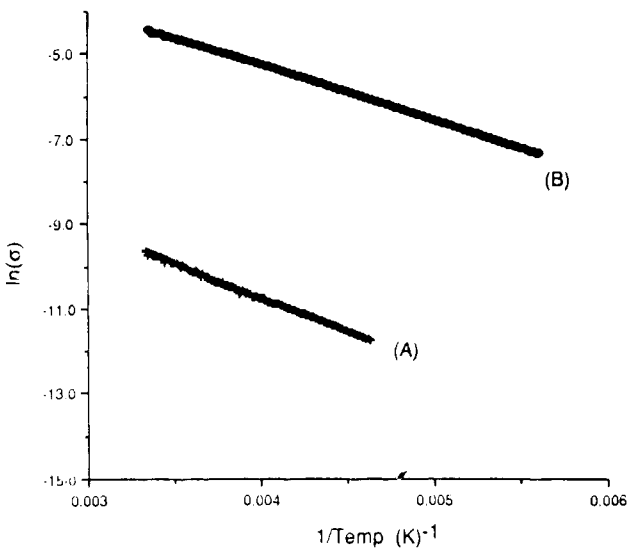

Figure 8. Plot of ln (conductivity) vs T^{-1}: (A) SnS_2, E_a = 0.14 eV; (B) $SnS_2\{CoCp_2\}_{0.31}$, E_a = 0.11 eV.

eV for SnS_2 and 0.11 eV for $SnS_2\{CoCp_2\}_{0.31}$. However, the room-temperature conductivity increases dramatically on intercalation from 6.0×10^{-5} $(\Omega\ cm)^{-1}$ for SnS_2 to 1.2×10^{-2} $(\Omega\ cm)^{-1}$ for $SnS_2\{CoCp_2\}_{0.31}$.

Mössbauer Spectroscopy. The ^{119}Sn Mössbauer spectra and computer fits are shown in Figure 9. Two resonances are observed in the sample that was ground under liquid nitrogen, and an additional resonance is discernible from the air-ground sample. The spectral parameters from the fits are listed in Table IV. Also given are parameters from unintercalated SnS_2.

The Sn^{4+} site has a slightly positive isomer shift and a slightly broader linewidth in the intercalated material relative to pure SnS_2. This may be the result of a slight change in the average Sn–S bond

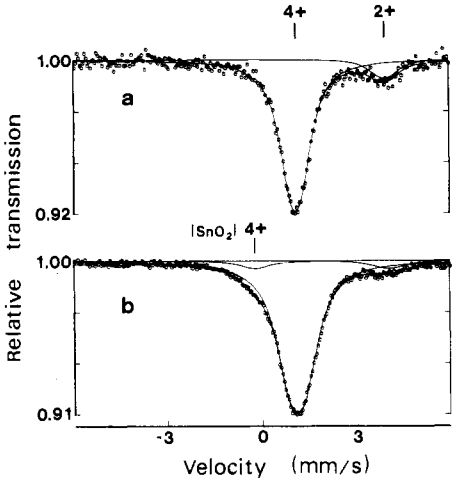

Figure 9. Mössbauer spectra of $SnS_2\{CoCp_2\}_{0.31}$: (a) sample ground under liquid nitrogen; (b) sample ground in air. The solid line passing through the data points is a least-squares fit of the superposition of Lorentzian-shaped lines indicated.

Table IV. Mössbauer Spectral Parameters for $SnS_2\{CoCp_2\}_{0.31}$ at Liquid-Nitrogen Temperature with Uncertainties in the Last Significant Figure Given in Parentheses

sample	site	chem shift (δ), mm/s	line width (Γ), mm/s	F,[a] %
$SnS_2\{CoCp_2\}_{0.31}$[b]	Sn^{4+}	1.09 (1)	1.05 (2)	90 (1)
	Sn^{2+}	4.00 (5)	1.0 (1)	10 (1)
$SnS_2\{CoCp_2\}_{0.31}$[c]	Sn^{4+}	1.14 (1)	1.35 (1)	91 (1)
	Sn^{2+}	4.0 (1)	1.0 (1)	5 (1)
	Sn^{4+}[d]	−0.1 (1)	0.9 (1)	4 (1)
SnS_2[e]	Sn^{4+}	1.05 (1)	0.92 (1)	100
SnS_2[f]	Sn^{4+}	1.06	0.96	100

[a] Fractional resonance area (integrated intensity). [b] Ground under liquid nitrogen. [c] Ground in air. [d] Sn^{4+} in SnO_2. [e] This work. [f] Reference 24a; at 93 K relative to $BaSnO_3$.

length and the creation of a distribution in bond lengths, induced by the intercalation. The Sn^{2+} site is readily identified by the large isomer shift characteristic of highly ionic divalent tin compounds such as $SnCl_2$ and $SnBr_2$.[23] The observed Sn^{2+} site has a larger isomer shift that those of Sn^{2+} in SnS or Sn_2S_3 and does not exhibit the large quadrupole splitting of Sn^{2+} in SnS or Sn_2S_3.[24] If one assumes that one electron has been transfered per cobaltocenium intercalated (67–74% of cobalt from XPS and 78% from magnetism), then about 9–11% of the Sn^{4+} sites would be reduced to divalent Sn sites. This is in good agreement with the 10% fractional resonance of Sn^{2+} in the liquid-nitrogen-ground specimen.

The air-sensitive nature of $SnS_2\{CoCp_2\}_{0.31}$ indicated by the XPS data is confirmed by the Mössbauer results from the sample ground in air: the Sn^{2+} is partially converted to an oxidized state with parameters similar to those of Sn^{4+} in SnO_2.[23] The air-ground sample also exhibited a more positive isomer shift and a much increased line width for the Sn^{4+} site. This indicates a grinding-induced Sn site disordering. If the broadened line is fitted with a quadrupole pair, then a splitting of 0.49 mm/s with a line width of 1.05 mm/s is obtained.

Conclusion

Changes in the electronic structure of both the host and guest upon intercalation is of interest in order to better understand intercalation reactions. For the layered metal dichalcogenides a transfer of electrons from intercalate electron states of low ionization potential to empty electron states of the guest material

(23) Flinn, P. A. In *Mossbauer Isomer Shifts*; Shenoy, G. K., Wagner, F. E., Eds.; North-Holland: New York, 1978; p 593.
(24) (a) Ichiba, S.; Kataba, M.; Negita, H. *Chem. Lett.* **1974**, 979. (b) Fano, V. *J. Chem. Phys.* **1975**, *61*, 5017.
(25) Diamagnetic correction equal to -124.5×10^{-6} emu mol^{-1}.
(26) Reference 3; p 260.

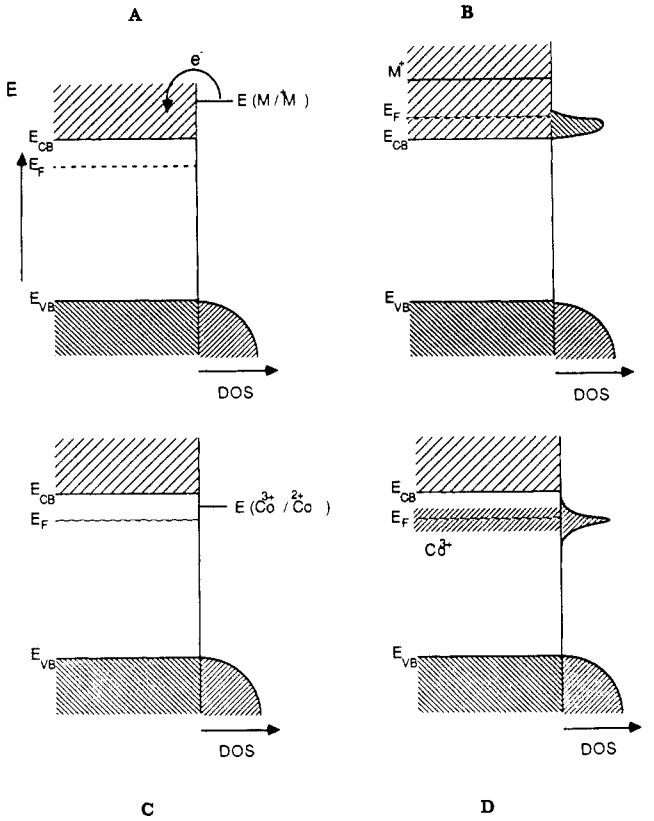

Figure 10. Proposed energy level diagram for cobaltocene and metal intercalation into SnS_2 (see text for explanation).

is usually postulated.[3] A semiconducting host material would become metallic if the conduction band is highly populated with electrons. Alkali-metal atoms, for example, have ionization potentials or reduction potentials far above the electron affinity of the solid, and complete electron transfer of the valence electron occurs and an intercalated M^+ species is formed (Figure 10A,B). The empty electron states of the alkali-metal s electrons are above the Fermi level of the solid and do not influence the electronic properties of the solid. However, for the case of less reducing metallocenes, intercalation is only possible if the ionization potential is above a certain threshold,[3] resulting in a smaller driving force for the redox process. For example we were unable to intercalate ferrocene or decamethylferrocene into SnS_2.

The overall driving force of a redox process is defined by the difference in the electrochemical potentials of the involved half-cell reactions. For the reducing guest species the electrochemical standard potential must be corrected for interactions with the solid, which in most cases is an unknown quantity. The electrochemical potential of the electrons in the solid is equivalent to the position of the Fermi level, which for semiconductors is very sensitive to the number of charge carriers at the band edges, e.g. electrons in the conduction band for n-type materials.

The presence of two different oxidation states of cobaltocene intercalated in SnS_2 suggests that the reduction potential is very close to the Fermi level of the semiconductor and the relative amount of reduced and oxidized species is determined by an electronic equilibrium with the Fermi level of the solid. From the electron affinity of SnS_2, determined from UV-photoemission spectroscopy as 4.2 eV,[27] and the activation energy of 0.15 eV from the temperature dependence of the conductivity of the n-doped SnS_2, the Fermi level is determined to be at an absolute potential of ca. 4.4 eV. This value corresponds to an electrochemical potential of −0.1 V vs the normal hydrogen electrode (NHE),[28] which is consistent with flatband measurements on the material in solutions of neutral pH.[29] The standard oxidation potential of $CoCp_2$ has been determined in organic solutions to be between −1.2 and −1.5 V vs NHE.[30]

The difference in the electrochemical potential within the lattice and in solution is related to the driving force for the reaction or the maximum open-circuit voltage obtainable from an intercalation battery constructed with these materials. The influence of the solid host on the redox potentials of the intercalate may result in substantial potential shifts. We propose an energy scheme as given in Figure 10C,D to describe the intercalation process.

In the literature there are two models for the bonding of intercalates and host lattices, which can be generally described as the weak covalent[31,32] and ionic[33,34] models. In the ionic model the stabilization of the charged species, which result from protonation and ionization with donation of an electron to the lattice, comes from solvation of the charged species by neutral guest molecules as is postulated for $TaS_2(NH_4^+)_{0.1}(NH_3)_{0.9}$.[34] The source of protons is from molecular decomposition or from impurities such as water. In our case the number of intercalated charged species outnumbers the neutral species (since the amount of intercalated solvent is minimal), so solvation effects would not seem to be operative.

If our generalized energy level picture for intercalation is correct then the equilibrium constant for the guest/$[guest]^+$ reaction would be a function of both the redox potential of the guest molecule and the position of the Fermi level in the host. We have attempted to test this hypothesis in this context by reacting SnS_2 with $CrCp_2$ (more reducing than $CoCp_2$) and $FeCp_2$ (less reducing than $CoCp_2$). Unfortunately $FeCp_2$ does not intercalate by direct reaction with SnS_2, and $CrCp_2$ reacts chemically with SnS_2.

In conclusion, from the combination of different measurements, we can formulate the SnS_2 cobaltocene intercalation compound as a remarkable mixed-valent compound in both tin and cobalt with an approximate formula $(Sn^{4+}_{0.9}Sn^{2+}_{0.1})S_2[[Co^{3+}Cp_2]^+_{0.2}[Co^{2+}Cp_2]_{0.1}]$.

Acknowledgment. We thank W. R. Bachman, L. Firment, S. McLean, and D. Wipf for their technical assistance.

Registry No. $SnS_2[CoCp_2]_{0.31}$, 56992-19-9; $CoCp_2$, 1277-43-6; $[CoCp_2]^+[PF_6]^-$, 12427-42-8; SnS_2, 1315-01-1.

(27) Williams, R. H.; Murray, R. B.; Govan, D. W.; Evans, E. L. *J. Phys. Chem.* **1973**, *6*, 3631.
(28) Frumkin, A. N.; Damaskin, B. B. *Dokl. Acad. Nauk SSSR.* **1975**, *221*, 395.
(29) Katty, A.; Fotouhi, B.; Gorochov, O. *J. Electrochem. Soc.* **1984**, *131*, 2806.
(30) Koelle, U.; Khouzami, F. *Angew. Chem., Int. Ed. Engl.* **1980**, *19*, 640.
(31) Betz, G.; Tributsch, H. *Prog. Solid State Chem.* **1986**, *16*, 195.
(32) Gamble, F. R.; Osiecki, J. H.; M. Cias, Pisharody, R.; DiSalvo, F. J.; Geballe, T. H. *Science (Washington, D.C.)* **1971**, *174*, 493.
(33) Gamble, F. R.; Osiecki, J. H.; DiSalvo, F. J. *J. Chem. Phys.* **1971**, *55*, 3525.
(34) Schöllhorn, R.; Zayefka, H. D. *Angew. Chem., Int. Ed Engl.* **1977**, *16*, 199.
(35) Johnston, J. W. *Physica B+C (Amsterdam)* **1980**, *99B+C*, 141.